

Effect of Compressed CO<sub>2</sub> on Phase Transitions and Polymorphism in Syndiotactic Polystyrene<sup>†</sup>

Y. Paul Handa,\* Zhiyi Zhang, and Betty Wong

Institute for Chemical Process and Environmental Technology,  
National Research Council of Canada, Ottawa, Ontario, Canada K1A 0R6Received August 12, 1997; Revised Manuscript Received October 16, 1997<sup>®</sup>

**ABSTRACT:** When treated with compressed CO<sub>2</sub>, syndiotactic polystyrene (sPS) undergoes a number of solid–solid transitions that do not occur on treatment with liquid solvents. For example, planar mesophase  $\rightarrow \beta$ ,  $\alpha \rightarrow \beta$ , and  $\gamma \rightarrow \beta$  transitions can be brought about under appropriate conditions of temperature and CO<sub>2</sub> pressure. In addition, the transitions of glassy sPS to the planar mesomorphic and to the  $\alpha$  form, and the  $\gamma \rightarrow \alpha$  transition occur at temperatures lower than when the same transitions are effected under ambient pressure. The dissolved CO<sub>2</sub> lowers the glass transition and the cold crystallization temperatures of sPS at the rate of  $-0.92$  and  $-0.58$  °C/atm, respectively. Crystallization kinetics from the sPS–CO<sub>2</sub> solution follow the Avrami equation, but the value of the exponent  $n$  is lower than when crystallization is conducted under ambient pressure.

## Introduction

Syndiotactic polystyrene (sPS) is a semicrystalline polymer, first synthesized in the mid-1980s using a homogeneous Ziegler–Natta catalyst.<sup>1,2</sup> It has good temperature and chemical resistances and is a potential engineering thermoplastic due to favorable crystallization kinetics and a wide processing window.<sup>3,4</sup> The crystallization rate of sPS from the melt is about 2 orders of magnitude higher than that of isotactic polystyrene under similar supercooling conditions<sup>5</sup> and it can attain crystallinity levels up to 70% with a melting point close to 270 °C.<sup>6,7</sup> There are four types of crystalline form,  $\alpha$ ,  $\beta$ ,  $\gamma$ , and  $\delta$ , and two types of mesomorphic form. Forms  $\alpha$  and  $\beta$  have T<sub>4</sub> conformation (zigzag chains) with an identity period of 5.1 Å,<sup>1,8,9</sup>  $\gamma$  and  $\delta$  have T<sub>2</sub>G<sub>2</sub> conformation (s(2/1)2 helical chains) with an identity period of 7.7 Å,<sup>10–12</sup> while the mesomorphic form can have T<sub>4</sub> or T<sub>2</sub>G<sub>2</sub> conformation depending on the morphology of the starting material used.

On heating, sPS undergoes a glass transition at about 95 °C and a cold crystallization at about 135 °C to give the planar mesomorphic phase, which serves as a template for growth of the  $\alpha$  form.<sup>8</sup> The latter form can also be obtained by rapid cooling from the melt state<sup>8</sup> or on heating the helical mesomorphic,  $\delta$ , or  $\gamma$  form.<sup>9,13,14</sup> The  $\beta$  form can be obtained by slow cooling from the melt or by casting from a solution in *o*-dichlorobenzene at elevated temperatures.<sup>15</sup> Depending on the solvent type, crystal form  $\delta$  or  $\gamma$  is obtained when amorphous sPS is immersed in liquid solvent and then dried under vacuum or directly exposed to solvent vapor.<sup>16–18</sup> Generally, the  $\delta$  form contains solvent molecules entrapped in the crystal structure whereas the  $\gamma$  form is free of solvent.<sup>7,19</sup> The mesophase with the helical conformation is obtained by removing the solvent molecules from the  $\delta$ -form,<sup>13,14</sup> and the mesophase with the zigzag conformation is obtained by annealing<sup>20</sup> or stretching<sup>21</sup> amorphous sPS above its  $T_g$ .

Certain transitions exist within the complex polymorphism exhibited by sPS. Due to the higher stability of the T<sub>4</sub> conformation than the T<sub>2</sub>G<sub>2</sub> conformation,<sup>22</sup>  $\gamma$  and

$\delta$  forms can undergo transitions to give the  $\alpha$  form but rarely the  $\beta$  form. On heating, the  $\delta$  form transforms to the helical mesophase around 90 °C and then to the  $\gamma$  form around 120 °C, which then transforms to the  $\alpha$  form around 190 °C.<sup>9,13,23–25</sup> Under a tensile force of about 14 MPa, the transition from  $\gamma$  to  $\alpha$  occurs at a much reduced temperature of 130 °C.<sup>26</sup> There is also one report on the direct transition from  $\delta$  to  $\beta$  form brought about by rapidly heating the  $\delta$  form to 160 °C.<sup>9</sup> The T<sub>4</sub>-based mesophase can directly transform to  $\alpha$  form on thermal annealing in the range 120–220 °C,<sup>20</sup> whereas the T<sub>2</sub>G<sub>2</sub>-based mesophase first transforms to the  $\gamma$  form before giving the  $\alpha$  form.<sup>13,14</sup> All these solid–solid transitions are irreversible due to the lower energy state of the T<sub>4</sub> conformation. A schematic representation of the main features of the polymorphism in sPS is given in Figure 1; a more detailed representation is reported elsewhere.<sup>27</sup>

The interactions with solvent molecules play a vital role in the complex polymorphism exhibited by sPS. It is well-known that the sorption of low molecular weight species leads to an acceleration of relaxation times of the macromolecules. This plasticization effect leads to lowering of the energy barriers, thereby making solid–solid and other transitions possible at much reduced temperatures. Recently, it has been shown that supercritical fluids or compressed gases, such as CO<sub>2</sub>, are also effective plasticizers for polymers.<sup>28–31</sup> Consequently, a polymer can crystallize at a temperature below its nominal  $T_g$  when contacted with supercritical fluids.<sup>32–38</sup> Unlike liquid solvents and vapors, the activity of a supercritical fluid can be changed continuously by simply changing its pressure. Furthermore, fluids like CO<sub>2</sub> are easily removed from the polymer matrix by depressurizing the system, thus making them better candidates to change the polymer morphology. In this context, the treatment of sPS with CO<sub>2</sub> in the supercritical or compressed gas state can be expected to produce morphological changes similar to those induced by treatments with liquids or vapors. In this paper we report a systematic investigation on the morphological modifications induced in sPS after treatment with CO<sub>2</sub> at various temperatures and pressures.

## Experimental Section

Syndiotactic polystyrene was provided by Prof. Michael Baird, Queen's University, Kingston, Ontario. It was purified

<sup>†</sup> Issued as NRCC No. 37643.

\* Author for correspondence; paul.handa@nrc.ca.

<sup>®</sup> Abstract published in *Advance ACS Abstracts*, December 15, 1997.

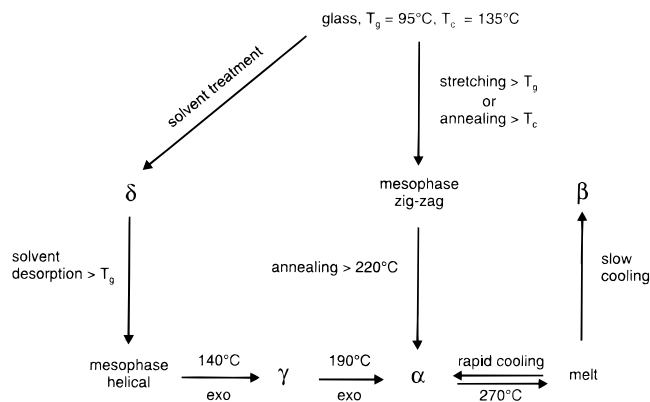


**Figure 1.** Schematic representation of the main features of polymorphism in sPS.

by first dissolving in 1,2,4-trichlorobenzene at 130 °C and then precipitating it by filtering the hot solution through a fritted glass funnel into a 1% HCl in methanol solution. The white precipitate was washed several times with methanol to get rid of any trace of trichlorobenzene. The sample was then vacuum dried at 100 °C for 24 h. Any atactic polystyrene was removed using methyl ethyl ketone in a Soxhlet extractor. sPS thus obtained was vacuum dried for 5 days. The final sample had a white cottony appearance. The sample was melt pressed at 300 °C and subsequently quenched in ice water to obtain 130  $\mu\text{m}$  thick films. X-ray analysis revealed the films to be completely amorphous.

For CO<sub>2</sub> treatments, a stainless steel VCR fitting with a volume of about 5 mL was used as the sample cell. It was connected through flexible tubing to a 150 mL gas reservoir kept at 35 °C. After the sample was installed in the cell, the system was evacuated for 15 min and then pressurized with CO<sub>2</sub>. When the desired pressure was achieved, the sample cell was placed in a Thermacraft furnace held at the required temperature and kept under the constant temperature and pressure conditions for 1 h. The cell was then taken out of the furnace and quenched to room temperature, followed by a slow depressurization of the system. The final samples used for DSC and X-ray analysis did not contain any CO<sub>2</sub>.

A SCINTAG diffractometer (Model XDS 2000) equipped with a graphite monochromator and a Cu K $\alpha$  radiation source was used to analyze the semicrystalline samples. The experiments were carried out at room temperature, and a scan rate of 4°/min was chosen for all measurements. Thermal analysis was done using a TA Instruments DSC 2910. All samples were scanned at 10 °C/min in a dry nitrogen environment. In-situ measurements of CO<sub>2</sub>-induced glass transition and crystallization were carried out using a Setaram DSC 121. Unlike conventional DSCs, this machine has a rather massive furnace with two symmetrical cavities containing the reference and sample vessels. A sample size up to 100 mg can be used, and the vessels are rated to 100 atm. The experimental details, calibration of the temperature and energy scales, and the technique used for making high-pressure calorimetric measurements are described elsewhere.<sup>39</sup> Briefly, after installing the sPS film, the system was evacuated for 1 h, and then both reference and sample sides were pressurized with CO<sub>2</sub> to the desired value and held at 35 °C for 1 h to allow the polymer-gas system to reach equilibrium. While still in contact with the gas, the sample was scanned from 20 to 200 °C for nonisothermal measurements or rapidly brought to 122 °C and held at this temperature for enough time to record the heat flow signal associated with isothermal crystallization kinetics.

## Results and Discussion

**Plasticization and Crystallization Kinetics.** Figure 2 shows the in-situ DSC scans of the sPS-CO<sub>2</sub> system at various pressures of CO<sub>2</sub>. For neat sPS, a glass transition at 97 °C and a cold crystallization temperature around 132 °C were observed. On saturation with CO<sub>2</sub>, both the glass transition and the crystal-

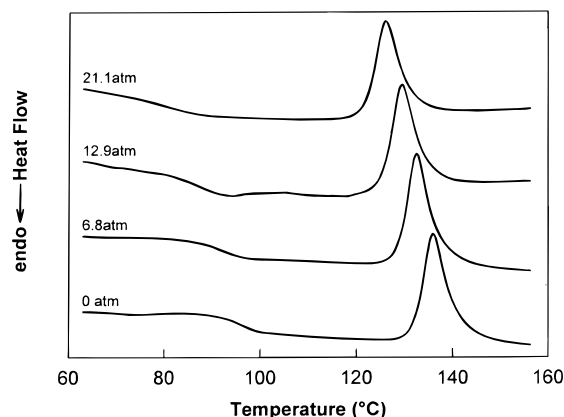


**Figure 2.** DSC traces of sPS scanned under various CO<sub>2</sub> pressures. Glassy sPS was first saturated with CO<sub>2</sub> at 35 °C and the pressures indicated before scanning.

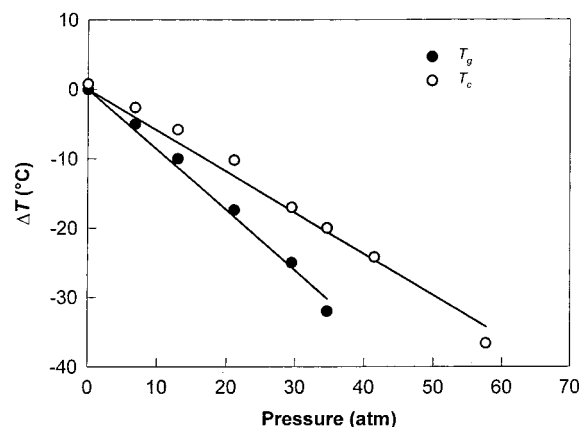


**Figure 3.** Depression in the glass transition temperature ( $T_g$ ) and the cold crystallization temperature ( $T_c$ ) of sPS as a function of CO<sub>2</sub> pressure.

lization events move to lower temperatures, and the glass transition becomes sluggish. The plasticization effect of CO<sub>2</sub> on sPS is similar to those observed in other polymer-CO<sub>2</sub> systems,<sup>28–31,39</sup> whereas the depression in crystallization temperature is similar to that reported for poly(*p*-phenylene sulfide)-CO<sub>2</sub>.<sup>35</sup> The depressions in  $T_g$  and the cold crystallization temperature  $T_c$  for sPS-CO<sub>2</sub> are plotted against the CO<sub>2</sub> pressure  $p$  in Figure 3. Both  $T_g$ - $p$  and  $T_c$ - $p$  curves are linear with slopes of  $-0.92$  and  $-0.58$  °C/atm, respectively. Thus, the decrease in crystallization temperature can be considered to arise primarily from the plasticization effect of CO<sub>2</sub>.

The plasticization of sPS by CO<sub>2</sub> also affects the isothermal crystallization kinetics. In Figure 4 are shown results for the fractional crystallinity induced as a function of time at 122 °C and various pressures. As seen in the figure, the crystallization of sPS is significantly accelerated even at the lowest pressure at which the polymer was saturated with CO<sub>2</sub>, and an almost 13-fold increase is achieved at a pressure of 30 atm. At 41 atm, the kinetics were so fast that the complete crystallization peak could not be recorded, as the polymer had already achieved maximum crystallinity before the temperature of the DSC could be stabilized. The crystallization kinetics were analyzed using the Avrami equation,<sup>5,40</sup>

$$\log[-\ln(1 - X_t)] = n \log(t - t_i) + \log K \quad (1)$$

where  $X_t$  is the extent of crystallinity induced at time  $t$ ,

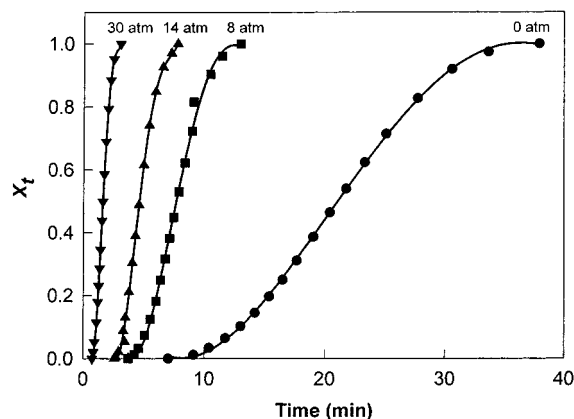


**Figure 4.** Crystallization isotherms of sPS at 122 °C under various CO<sub>2</sub> pressures. Glassy sPS was first saturated with CO<sub>2</sub> at 35 °C and the pressures indicated before being brought to the crystallization temperature. Curves are drawn through the data points to show the trend.

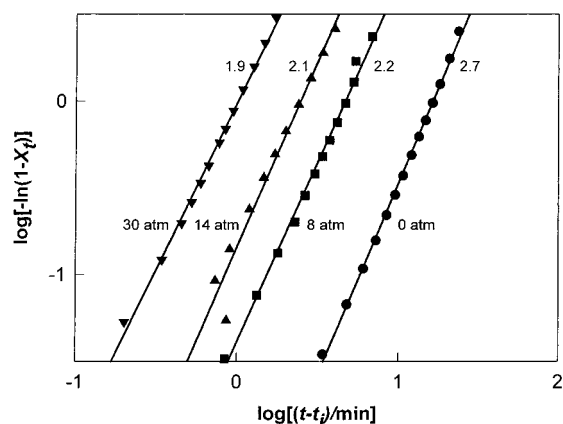


**Figure 5.** Avrami plots for sPS at 122 °C. Each curve is labeled with the CO<sub>2</sub> pressure of treatment and the Avrami exponent  $n$ . Lines through the data points are the fits according to eq 1.

$t_i$  is the induction time for nucleation,  $n$  is the Avrami exponent and reflects the mechanism of nucleation and crystal growth, and  $K$  is the kinetic rate constant for nucleation and growth. Avrami plots for sPS–CO<sub>2</sub> are shown in Figure 5; values of  $n$  pertaining to various treatment conditions are shown on each curve. For neat sPS, the value 2.7 for  $n$  obtained in this work is similar to the values between 2 and 3 reported in the literature.<sup>5</sup> On treatment with CO<sub>2</sub>,  $n$  tends to decrease, suggesting a possible change in nucleation type or crystal growth geometry.<sup>40</sup> It should be noted that under the  $T$  and  $p$  conditions used for investigating isothermal crystallization, the crystalline form of sPS is the same, *i.e.*, the planar mesophase (see below).

**Crystallization from the Glassy State.** Figures 6 and 7 show the wide angle X-ray diffraction patterns and DSC scans, respectively, for sPS annealed at various temperatures and ambient pressure for 1 h. For the sample annealed at 90 °C, the diffraction pattern is that of glassy sPS<sup>9,14</sup> and the thermal scan shows the typical enthalpy relaxation peak just after the glass transition at 97 °C and the cold crystallization and melting events with peak temperatures at about 132 and 277 °C, respectively. At 130 °C, a temperature within the cold crystallization region of amorphous sPS, the diffraction pattern is that of the planar mesomorphic phase with T<sub>4</sub> conformation.<sup>14,20,31</sup> At 175 and 210 °C, the pattern is essentially that of the mesophase with a hint of the evolution of the  $\alpha$  phase. The  $\alpha$  phase,

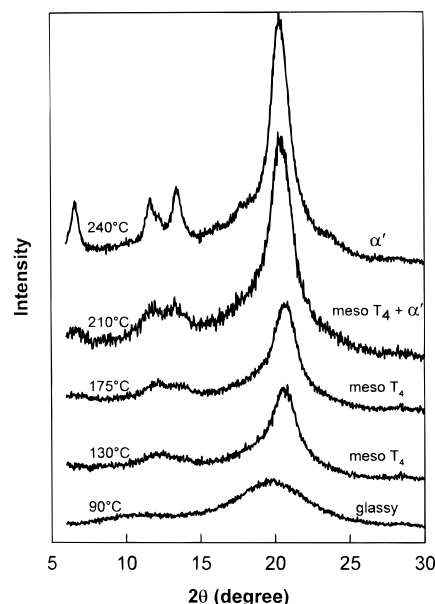


**Figure 6.** X-ray diffraction patterns of glassy sPS annealed under ambient pressure and the various temperatures for 1 h. Each pattern is also labeled with the phase(s) identified.

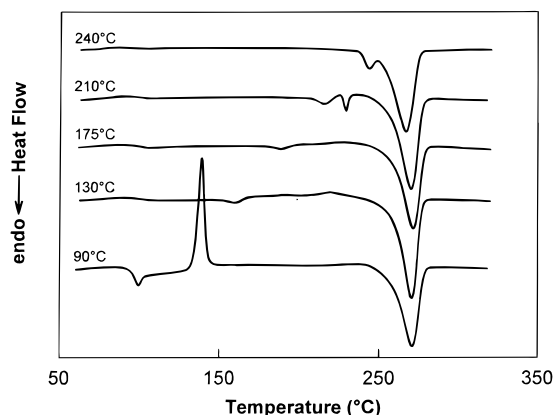


**Figure 7.** DSC traces of glassy sPS annealed under ambient pressure and the various temperatures for 1 h.

however, is fully formed at 240 °C; the crystals obtained under such conditions generally show broad reflections and have a low degree of perfection, and the crystalline phase is termed  $\alpha'$ .<sup>9,41</sup> For the samples annealed at 130 and 175 °C, the DSC scans show small endotherms at temperatures slightly higher than the annealing temperatures. These endotherms are associated with reorganization within the mesophase. For the sample annealed at 210 °C, again an endotherm for the reorganization of the mesophase is seen at 218 °C followed immediately by another endotherm associated with perfection of the  $\alpha$  crystals thus formed. The latter phenomenon is also seen for the sample annealed at 240 °C where the double melting behavior is due to melting of the less ordered crystals ( $\alpha'$  crystals), followed immediately by the melting of the  $\alpha$  phase. The results shown in Figures 6 and 7 are in agreement with previous studies<sup>20,31,41</sup> which showed that on annealing sPS in the range 120–220 °C, the planar mesophase is nucleated first, which then converts into the poorly ordered  $\alpha'$  form. The extent of conversion depends on the annealing temperature and time. The complete conversion takes place at temperatures above 220 °C. Thus, during a DSC scan, the mesophase is gradually converted into the  $\alpha$  form, and no distinct thermal event pertaining to such a transformation is observed.

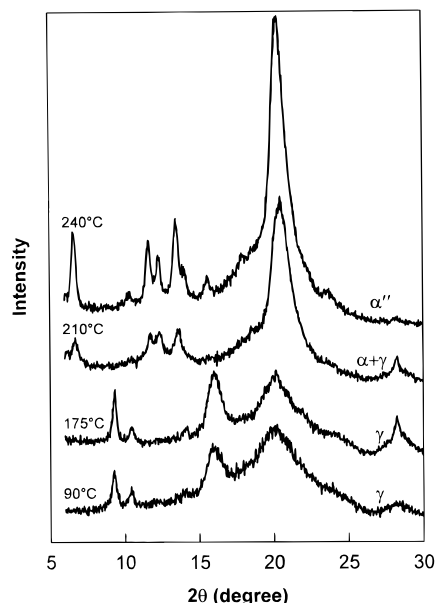


**Figure 8.** X-ray diffraction patterns of glassy sPS treated with 57 atm CO<sub>2</sub> at the various temperatures shown. Each pattern is also labeled with the phase(s) identified.

When the same thermal treatments as those described in Figures 6 and 7 are carried out in the presence of CO<sub>2</sub> at 57 atm, we obtain dramatically different results. The X-ray diffraction patterns for various such treatments are shown in Figure 8. For the annealing temperatures of 90 and 175 °C, the structure obtained is that of the  $\gamma$  form.<sup>9,14,19</sup> It should be noted that the  $\gamma$  form has usually been obtained by first crystallizing sPS into the  $\delta$  form using an appropriate liquid solvent and then transforming it into the  $\gamma$  form via the mesophase, (Figure 1). The  $\gamma$  form can also be obtained directly by treating the glassy sPS with acetone and then removing the solvent by thermal/vacuum techniques.<sup>12</sup> With CO<sub>2</sub>, glassy sPS is directly transformed into the  $\gamma$  form. Furthermore, on depressurization, CO<sub>2</sub> escapes from the polymer matrix and, thus, no desorption step is required.

On heating, the  $\gamma$  form transforms to the  $\alpha$  form at about 190 °C.<sup>9,13,14,23–25</sup> Consequently, as seen in Figure 8, the sample treated at 210 °C and 57 atm gives a pattern typical of the  $\alpha$  form. However, there is still a peak at  $2\theta = 28.2^\circ$ , reflecting the presence of a small amount of the  $\gamma$  form. At the higher treatment temperature of 240 °C, the structure obtained is that of the  $\alpha$  form with no trace of the  $\gamma$  form, but this time the pattern is quite different from that shown in Figure 6 and corresponds to that of the  $\alpha''$  form characterized by sharper reflections and a higher degree of crystal perfection.<sup>9,41</sup> The formation of more perfect crystals with CO<sub>2</sub> treatment is also reflected by comparing the 240 °C labeled DSC scans in Figures 7 and 9; the CO<sub>2</sub>-treated crystals (Figure 9) melt with a single, sharper peak, whereas the thermally treated crystals (Figure 7) melt with a broad, double peak. For the other scans shown in Figure 9, again the small endotherms observed at temperatures slightly higher than the annealing temperatures are due to reorganization within the  $\gamma$  form, and the small exotherms that follow are due to the  $\gamma \rightarrow \alpha$  transition.<sup>13,14</sup> The latter transition moves to higher temperatures as the annealing temperature is raised. Consequently, this transition is not observed in the sample annealed at 210 °C as at this temperature only a small amount of the  $\gamma$  form is present and the

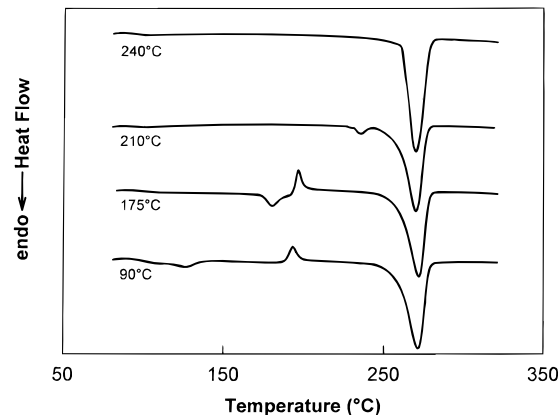


**Figure 9.** DSC traces of glassy sPS treated with 57 atm CO<sub>2</sub> at the various temperatures shown. After treatment, the samples were cooled to room temperature, degassed, and then scanned under ambient pressure.

delayed  $\gamma \rightarrow \alpha$  transition is smeared out by the main melting peak.

It should be noted that the  $\alpha''$  form has previously been obtained only through melt-crystallization<sup>9,41</sup> whereas the results in Figure 8 show that it can be obtained directly from the glassy state. This indicates that the plasticization by CO<sub>2</sub> provides the macromolecules with relaxation times essentially similar to those available in the melt state. The results shown in Figures 8 and 9 were obtained when sPS was treated with 57 atm CO<sub>2</sub>. However, a treatment with 40 atm CO<sub>2</sub> in the temperature range 90–130 °C produced only the planar mesophase similar to that obtained by annealing at 130 °C under ambient pressure (Figure 6). Thus, the extent of plasticization plays an important role in determining the resulting morphology. For example, when amorphous sPS was treated at a lower pressure of 29 atm and at 210 and 240 °C, the  $\alpha'$  form with diffraction patterns similar to that shown for 240 °C in Figure 6 was obtained due to the insufficient plasticization effect. The DSC scans on these samples gave small endotherms before the main melting peak, these endotherms occurring at temperatures higher than those for the similar endotherms in the 210 and 240 °C treated samples in Figure 7. This indicates that the  $\alpha$  form contained crystallites larger than those obtained without using CO<sub>2</sub> but smaller than those obtained on treatment at a higher pressure of CO<sub>2</sub>.

On the other hand, when CO<sub>2</sub> at a pressure of 122 atm was used during the thermal annealing at 210 and 240 °C, amorphous sPS transformed directly into the  $\beta$  form instead of into the  $\alpha$  form. The results are shown in Figure 10. At 240 °C, the diffraction pattern obtained is similar to that when the  $\beta$  form is crystallized from the melt.<sup>9,15</sup> A small peak at  $2\theta = 28.2^\circ$  is present in the sample treated at 210 °C but absent in that treated at 240 °C and, based on the results shown in Figure 8, can be attributed to the presence of a small amount of the  $\gamma$  form. In going from 210 to 240 °C, the fine structure of the  $\beta$  form develops, as indicated by the appearance of a peak at  $2\theta = 21.3^\circ$ ,<sup>15</sup> and its crystallinity also increases, as indicated by the increase in diffraction intensity. However, the  $\beta$  form obtained still corresponds to the low-order phase  $\beta'$ ; the more ordered phase  $\beta''$  is characterized by additional peaks at  $2\theta = 13.6$  and  $15.8^\circ$ .<sup>15</sup> The DSC scans on these samples showed small endotherms before the main melting peak. These are reminiscent of the structural reorganization process similar to the ones discussed above for the mesomorphic,  $\gamma$ , and  $\alpha$  phases.

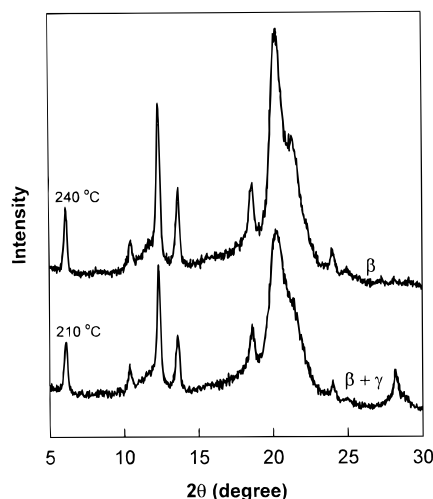


**Figure 10.** X-ray diffraction patterns of glassy sPS treated with 122 atm CO<sub>2</sub> at the various temperatures shown. Each pattern is also labeled with the phase(s) identified.

It should be noted that previously the  $\beta$  form has never been obtained from the glassy state but only by either slow cooling from the melt or casting at elevated temperatures from a solution in *o*-dichlorobenzene or rapidly heating the  $\delta$  form to 160 °C.<sup>9,15</sup> Obviously, CO<sub>2</sub> is responsible for the direct transformation of glassy sPS into the  $\beta$  form. However, since the compressed gas also exerts hydrostatic pressure on the polymer, it is desirable to establish whether the CO<sub>2</sub>-induced transformation of glassy sPS into its  $\beta$  form is mainly due to the plasticization effect. The solubility of N<sub>2</sub> in polymers is generally quite low, and thus, compressed N<sub>2</sub> is expected only to exert hydrostatic pressure on the polymer. Consequently, amorphous sPS was treated at 240 °C with N<sub>2</sub> at 122 and 180 atm. In both cases, the crystalline structure obtained was the  $\alpha$  form, which as noted above, will form under ambient pressure as well. The hydrostatic pressure effect can, therefore, be considered to have a negligible effect in the transition from amorphous sPS to the  $\beta$  form, and the plasticization effect of CO<sub>2</sub> can be taken as the primary reason for the direct transformation to the  $\beta$  form. The crystallization rate constant for sPS increases rapidly with temperature, reaches a maximum value at about 190 °C and then drops sharply at higher temperatures.<sup>42</sup> In terms of the CO<sub>2</sub>-induced plasticization effect on  $T_g$  and  $T_c$  reported here in Figure 3 and on the melting temperature reported elsewhere,<sup>43</sup> such a concave curve will be expected to shift to lower temperatures when sPS is crystallized in the presence of CO<sub>2</sub>. Consequently, at temperatures above 200 °C, a lower crystallization rate will be expected, favoring, thus, the formation of the  $\beta$  form.

The results presented above show that the crystalline structure obtained from glassy sPS depends on the treatment conditions of temperature and pressure. Both parameters,  $T$  and  $p$ , affect the polymer in the same way—by accelerating the relaxation time or helping overcome the energy barrier to a given transition. As shown above, with increasing pressure, and thus with increasing CO<sub>2</sub> solubility, a given energy barrier can be overcome at a lower temperature. Nevertheless, there are limits to the extent the dissolved CO<sub>2</sub> can compensate for elevated temperature requirements. For example, the  $\gamma$  form cannot be obtained at low CO<sub>2</sub> pressure by just raising the temperature, while the  $\alpha$  form cannot be obtained at a temperature below the  $\gamma$

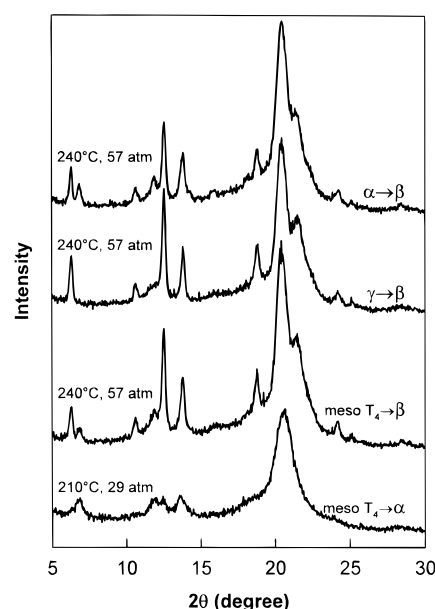


**Figure 11.** X-ray diffraction patterns of sPS treated at the various temperatures and CO<sub>2</sub> pressures shown. Each pattern is also labeled with structure of the starting and the resulting phase.

→  $\alpha$  transition temperature of around 190 °C by increasing the CO<sub>2</sub> pressure to even over 250 atm.

#### Transitions between Various Crystalline Forms.

There exist certain transitions between the various crystalline forms of sPS. In the presence of CO<sub>2</sub>, these solid–solid transitions can be induced at lower temperatures, and some new transitions, never observed before, can also be brought about. These results are shown in Figure 11 where each diffraction pattern is labeled with the temperature and pressure conditions of treatment and the starting phase and the arrow points to the resulting phase. As before, structural assignments were made on the basis of previous studies.<sup>9,15</sup> When crystallized samples are thermally annealed at ambient pressure, the  $\gamma$  →  $\alpha$  transition occurs at about 190 °C,<sup>9,13,14,23–25</sup> and the planar-mesomorphic →  $\alpha$  transition occurs in the range 120–220 °C.<sup>20,31,41</sup> The mesomorphic →  $\alpha$  transition temperature, however, is reduced when the sample is treated with CO<sub>2</sub> at relatively low pressures. As shown in Figure 11, a sample that was in the mesomorphic form (Figure 6, 130 °C) exhibits a typical  $\alpha$  form pattern after treatment at 210 °C and 29 atm CO<sub>2</sub>. When the same mesophase is treated at 240 °C and 57 atm CO<sub>2</sub>, a diffraction pattern for the  $\beta$  form is obtained. Again, as shown in Figure 11, a sample in the  $\gamma$  form (Figure 8, 175 °C) transformed to the  $\beta$  form on treatment at 240 °C and 57 atm. In fact, both the mesomorphic →  $\beta$  and  $\gamma$  →  $\beta$  transitions also occurred at a lower temperature of 210 °C. Surprisingly, an  $\alpha$  →  $\beta$  transition was observed when a sample in the  $\alpha$  form (Figure 6, 240 °C) was treated at 240 °C and 57 atm (Figure 11, top pattern). This  $\beta$  form has an extra peak at  $2\theta = 6.8^\circ$ , which is characteristic of the  $\alpha$  form, possibly due to the residual  $\alpha$  phase in the sample. In Figure 12, the various transitions induced by CO<sub>2</sub> are summarized, where the arrows show the transition direction, the dashed lines represent transitions that occur under both ambient pressures and in the presence of compressed CO<sub>2</sub> but at reduced temperatures, and the solid lines show transitions that are brought about only by compressed CO<sub>2</sub>.

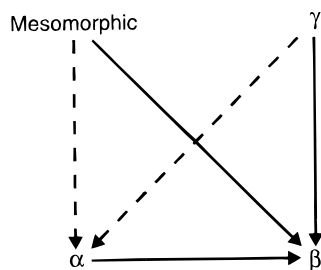


**Figure 12.** Various transitions made possible by treating sPS with compressed CO<sub>2</sub>. The arrows show the direction of the transition: solid arrows indicate transitions that only occur in the presence of CO<sub>2</sub>, and broken arrows indicate transitions that can occur under ambient pressure but also occur at reduced temperatures in the presence of compressed CO<sub>2</sub>.

A comparison of the results in Figures 8, 10, and 11, shows that the temperatures required for producing  $\alpha$  phase from mesomorphic or  $\gamma$  phase and for producing  $\beta$  phase from mesomorphic,  $\gamma$ , or  $\alpha$  phase are similar to those for producing  $\alpha$  and  $\beta$  phases directly from amorphous sPS. However, the treatment with compressed CO<sub>2</sub> allows formation of the  $\alpha$  and  $\beta$  phases through crystallization from the glassy state or through transition from a less stable form. The  $\alpha \rightarrow \beta$  transition, however, is quite intriguing considering that the temperature required for obtaining the original  $\alpha$  form is identical to that used for converting it to the  $\beta$  form on treatment with CO<sub>2</sub>. We have observed that, for semicrystalline polymers, CO<sub>2</sub> dissolved in the amorphous part lowers the melting temperature of the polymer crystals.<sup>43</sup> It is possible then that the  $\beta$  form grows out of the sPS-CO<sub>2</sub> solution in a manner similar to its growth from the pure melt on slow cooling. Whatever the mechanism, the CO<sub>2</sub> treatment provides new pathways to make the  $\beta$  form, which is the desirable of the two planar forms ( $\alpha$  and  $\beta$ ) because of its better mechanical properties and solvent resistance.<sup>8,44,45</sup>

The  $\alpha$  form transforms to the  $\delta$  form on exposure to dichloromethane.<sup>11,45</sup> This transition along with the possibility of obtaining the  $\gamma$  form from the  $\alpha$  form or the planar mesophase was also investigated by treating the samples at temperatures to 175 °C and pressures to 204 atm, but without success. The  $\delta$  form is stable only in the presence of enclathrated solvent molecules like CH<sub>2</sub>Cl<sub>2</sub>.<sup>9,13,14</sup> CO<sub>2</sub>, due to its higher diffusivity or the inability to complex with SPS, is not able to stabilize the  $\delta$  form. Both the  $\alpha$  and the mesomorphic forms have T<sub>4</sub> conformation and are in a lower energy state than the T<sub>2</sub>G<sub>2</sub> conformation based  $\gamma$  form.<sup>22</sup> Consequently, even with the plasticizing effect of CO<sub>2</sub>, it is not possible to overcome the energy barrier to go from the T<sub>4</sub> to T<sub>2</sub>G<sub>2</sub> conformation.

**Acknowledgment.** The authors thank Prof. Michael Baird for providing the sPS sample, Ms. Lisa-Renée Carriere for purifying it, and Dr. Isobel Davidson for assistance with the diffraction work.

## References and Notes

- (1) Ishihara, N.; Seimiya, T.; Kuramoto, M.; Uoi, M. *Macromolecules* **1986**, *19*, 2464.
- (2) Pellechia, C.; Longo, P.; Grassi, A.; Ammendola, P.; Zambelli, A. *Makromol. Chem., Rapid Commun.* **1987**, *8*, 277.
- (3) Pasztor, A. J.; Landes, B. G.; Karjala, P. J. *Thermochim. Acta* **1991**, *177*, 187.
- (4) Ishihara, N. *Macromol. Symp.* **1995**, *89*, 553.
- (5) Cimmino, S.; di Pace, E.; Martuscelli, E.; Silvestre, C. *Polymer* **1991**, *32*, 1080.
- (6) Filho, A. R.; Vittoria, V. *Makromol. Chem., Rapid Commun.* **1990**, *11*, 199.
- (7) Gianotti, G.; Valvassori, A. *Polymer* **1990**, *31*, 473.
- (8) Vittoria, V.; Russo, R.; de Candia, F. *J. Macromol. Sci., Phys.* **1989**, *B28*, 419.
- (9) Guerra, G.; Vitagliano, V. M.; de Rosa, C.; Petraccone, V.; Corradini, P. *Macromolecules* **1990**, *23*, 1539.
- (10) Vittoria, V.; de Candia, F.; Iannelli, P.; Immirzi, A. *Makromol. Chem., Rapid Commun.* **1988**, *9*, 765.
- (11) Immirzi, A.; de Candia, F.; Iannelli, P.; Zambelli, A. *Makromol. Chem., Rapid Commun.* **1988**, *9*, 761.
- (12) Vittoria, V.; Russo, R.; de Candia, F. *Polymer* **1991**, *32*, 3371.
- (13) de Candia, F.; Guadagno, L.; Vittoria, V. *J. Macromol. Sci., Phys.* **1995**, *B34*, 95.
- (14) Manfredi, C.; de Rosa, C.; Guerra, G.; Rapacciuolo, M.; Auriemma, F.; Corradini, P. *Macromol. Chem. Phys.* **1995**, *196*, 2795.
- (15) de Rosa, C.; Rapacciuolo, M.; Guerra, G.; Petraccone, V.; Corradini, P. *Polymer* **1992**, *33*, 1423.
- (16) Grassi, A.; Longo, P.; Guerra, G. *Makromol. Chem., Rapid Commun.* **1989**, *10*, 687.
- (17) de Candia, F.; Romano, G.; Russo, R.; Vittoria, V. *Colloid Polym. Sci.* **1993**, *271*, 454.
- (18) de Candia, F.; Carotenuto, M.; Guadagno, L.; Vittoria, V. *J. Macromol. Sci.-Phys.* **1996**, *B35*, 265.
- (19) Manfredi, C.; del Nobile, M. A.; Mensitieri, G.; Guerra, G.; Rapacciuolo, M. *J. Polym. Sci., Part B: Polym. Phys.* **1997**, *35*, 133.
- (20) de Candia, F.; Filho, A. R.; Vittoria, V. *Colloid Polym. Sci.* **1991**, *269*, 650.
- (21) de Candia, F.; Filho, A. R.; Vittoria, V. *Makromol. Chem., Rapid Commun.* **1991**, *12*, 295.
- (22) Doherty, D. C.; Hopfinger, A. J. *Macromolecules* **1989**, *22*, 2472.
- (23) Reynolds, N. M.; Savage, J. D.; Hsu, S. L. *Macromolecules* **1989**, *22*, 2867.
- (24) Reynolds, N. M.; Stidham, H. D.; Hsu, S. L. *Macromolecules* **1991**, *24*, 3662.
- (25) Wang, Y. K.; Savage, J. D.; Yang, D.; Hsu, S. L. *Macromolecules* **1992**, *25*, 3659.
- (26) de Candia, F.; Russo, R.; Vittoria, V. *Polym. Commun.* **1991**, *32*, 306.
- (27) Kellar, E. J. C.; Galiotis, C.; Andrews, E. H. *Macromolecules* **1996**, *29*, 3515.
- (28) Wang, W. C. V.; Kramer, E. J.; Sachse, W. H. *J. Polym. Sci., Polym. Phys. Ed.* **1982**, *20*, 1371.
- (29) O'Neill, M. L.; Handa, Y. P. *Assignment of the Glass Transition*; Seyler, R. J., Ed.; ASTM STP 1249; American Society for Testing and Materials: Philadelphia, 1994.
- (30) Handa, Y. P.; Lampron, S.; O'Neill, M. J. *Polym. Sci., Part B: Polym. Phys.* **1994**, *32*, 2549.
- (31) Handa, Y. P.; Kruus, P.; O'Neill, M. J. *Polym. Sci., Part B: Polym. Phys.* **1996**, *34*, 2635.
- (32) Chiou, J. S.; Barlow, J. W.; Paul, D. R. *J. Appl. Polym. Sci.* **1985**, *30*, 3911.
- (33) Beckman, E.; Porter, R. S. *J. Polym. Sci., Polym. Phys. Ed.* **1987**, *25*, 1511.
- (34) Mizoguchi, K.; Hirose, T.; Naito, Y.; Kamiya, Y. *Polymer* **1987**, *28*, 1298.
- (35) Schultze, J. D.; Engelmann, I. A. D.; Bohning, M.; Springer, J. *Polym. Adv. Technol.* **1991**, *2*, 123.
- (36) Lambert, S. M.; Paulaitis, M. E. *J. Supercrit. Fluids* **1991**, *4*, 15.
- (37) Handa, Y. P.; Capowski, S.; O'Neill, M. *Thermochim. Acta* **1993**, *226*, 177.
- (38) Handa, Y. P.; Roovers, J.; Wang, F. *Macromolecules* **1994**, *27*, 5511.
- (39) Zhang, Z.; Handa, Y. P. *J. Polym. Sci., Part B: Polym. Phys.*, in press.
- (40) Wunlich, B. *Macromolecular Physics*; Academic Press: New York, 1976; Vol. 2.
- (41) Vittoria, V.; Filho, A. R.; de Candia, F. *J. Macromol. Sci., Phys.* **1991**, *B30*, 155.
- (42) Wesson, R. D. *Polym. Eng. Sci.* **1994**, *34*, 1157.
- (43) Zhang, Z.; Handa, Y. P. *Macromolecules* **1997**, *30*, 8505.
- (44) de Candia, F.; Romano, G.; Russo, R.; Vittoria, V. *Colloid Polym. Sci.* **1990**, *268*, 720.
- (45) Rapacciuolo, M.; de Rosa, C.; Guerra, G.; Mensitieri, G.; Apicella, A.; del Nobile, M. A. *J. Mater. Sci. Lett.* **1991**, *10*, 1084.